HHS Public Access

Author manuscript

Hepatology. Author manuscript; available in PMC 2015 September 16.

Published in final edited form as:

Hepatology. 2013 August ; 58(2): 788–798. doi:10.1002/hep.26401.

Hepatocyte divalent metal-ion transporter-1 is dispensable for hepatic iron accumulation and non-transferrin-bound iron uptake in mice

Chia-Yu Wang and **Mitchell D. Knutson**

Food Science and Human Nutrition Department, University of Florida, Gainesville, FL 32611

Abstract

Divalent metal-ion transporter-1 (DMT1) is required for iron uptake by the intestine and developing erythroid cells. DMT1 is also present in the liver, where it has been implicated in the uptake of transferrin-bound iron (TBI) and non-transferrin-bound iron (NTBI), which appears in the plasma during iron overload. To test the hypothesis that DMT1 is required for hepatic iron uptake, we examined mice with the *Dmt1* gene selectively inactivated in hepatocytes ($Dmt1^{liv/liv}$). We found that $Dmt1^{liv/liv}$ mice and controls ($Dmt1^{flox/flox}$) did not differ in terms of hepatic iron concentrations or other parameters of iron status. To determine if hepatocyte DMT1 is required for hepatic iron accumulation, we crossed $Dmt1^{liv/liv}$ mice with $Hfe^{-/-}$ and hypotransferrinemic ($Trf^{hpx/hpx}$) mice that develop hepatic iron overload. Double-mutant $Hfe^{-/-}$;$Dmt1^{liv/liv}$ and $Trf^{hpx/hpx}$;$Dmt1^{liv/liv}$ mice were found to accumulate similar amounts of hepatic iron as did their respective controls. To directly assess the role of DMT1 in NTBI and TBI uptake, we injected ^{59}Fe-labeled ferric citrate (for NTBI) or ^{59}Fe-transferrin into the plasma of $Dmt1^{liv/liv}$ and $Dmt1^{flox/flox}$ mice and measured the uptake of ^{59}Fe by the liver. $Dmt1^{liv/liv}$ mice displayed no impairment of hepatic NTBI uptake, but TBI uptake was 40% lower. Hepatic levels of transferrin receptors 1 and 2 and ZIP14 (ZRT/IRT-like protein 14), which may also participate in iron uptake, were unaffected in $Dmt1^{liv/liv}$ mice. Additionally, liver iron levels were unaffected in $Dmt1^{liv/liv}$ mice fed an iron-deficient diet.

Conclusion—Hepatocyte DMT1 is dispensable for hepatic iron accumulation and NTBI uptake. Although hepatocyte DMT1 is partially required for hepatic TBI uptake, hepatic iron levels were unaffected in $Dmt1^{liv/liv}$ mice, suggesting that this pathway is a minor contributor to the iron economy of the liver.

Keywords

iron overload; hemochromatosis; thalassemia; DMT1; *SLC11A2*

Contact Information Mitchell D. Knutson, Food Science and Human Nutrition Department, PO Box 110370, University of Florida, Gainesville, FL 32611, Phone: (352) 392-1991 X 204, Fax: (352) 392 9436, mknutson@ufl.edu.

The authors have no conflicts of interest to declare.

INTRODUCTION

A typical adult male has roughly 4 g of total body iron, including about 1 g of iron stores (1). Approximately 25–50% of storage iron is found in the liver, mainly in hepatocytes and Kupffer cells. In iron overload disorders such as *HFE*-related hereditary hemochromatosis, hepatic iron stores increase over time, with iron depositing predominantly in hepatocytes (2, 3). Although hepatocytes comprise a major part of the iron storage system, exactly how these cells take up iron, particularly during iron overload, is not well understood. Under normal circumstances, hepatocytes in the liver can acquire iron from the plasma iron-transport protein transferrin (4). It is generally assumed that the uptake of transferrin-bound iron (TBI) by the liver involves the transferrin receptor (TfR1) endocytosis pathway (5). In this model, transferrin carrying up to two atoms of ferric iron (Fe^{3+}) binds to transferrin receptor (TfR1) at the hepatocyte cell surface, initiating the internalization of the transferrin/TfR1 complex into endosomes. Subsequent endosomal acidification causes transferrin to release its Fe^{3+}, which is then reduced to Fe^{2+} and transported into the cytosol via divalent metal-ion transporter-1 (DMT1).

DMT1 was first identified as a transmembrane iron-transport protein by Gunshin et al. (6) in 1997. Iron transport via DMT1 was demonstrated to be maximal at pH 5.5, and its expression was markedly induced in iron-deficient rat duodenum, suggesting that it functions in intestinal iron absorption. A common missense mutation in DMT1 was later found in the *mk* mouse and Belgrade rat (7), two animal models characterized by impaired iron absorption, reduced iron assimilation by developing erythroid cells, and anemia. Given that erythroid precursor cells exclusively take up iron from transferrin (8), it was proposed that DMT1 participates in TBI uptake (7). Formal proof that DMT1 plays a role in intestinal iron absorption and developing erythroid cells was provided by studies of mice in which DMT1 was inactivated in intestinal epithelial cells ($Dmt1^{int/int}$) and globally ($Dmt1^{-/-}$) (9).

As DMT1 is also expressed in the liver, it is often cited that DMT1 plays a role in hepatocyte iron metabolism (5, 10–17), either through the uptake of TBI or non-transferrin-bound iron (NTBI), which appears in the plasma during iron overload (18). However, no studies have directly tested the *in vivo* role of hepatocyte DMT1 in liver iron metabolism. We therefore examined mice with the *Dmt1* gene selectively inactivated in hepatocytes ($Dmt1^{liv/liv}$) and evaluated their hepatic as well as systemic iron status. To determine if DMT1 is required for hepatic iron accumulation during iron overload, we crossed $Dmt1^{liv/liv}$ mice with two genetic models of iron overload—*Hfe* knockout ($Hfe^{-/-}$) mice (3) and hypotransferrinemic ($Trf^{hpx/hpx}$) mice (19). Using the $Dmt1^{liv/liv}$ mice, we also directly assessed the requirement for DMT1 in the hepatic uptake of TBI and NTBI. We additionally examined the effect of iron deficiency on hepatic TBI uptake and iron status in $Dmt1^{liv/liv}$ mice.

EXPERIMENTAL PROCEDURES

Animals

$Hfe^{-/-}$ (20), $Dmt1^{flox/flox}$ and $Dmt1^{liv/liv}$ mice (9) were on the 129S6/SvEvTac background and $Trf^{hpx/hpx}$ mice were on the BALB/cJ background (19). Animal protocols were approved

by the Institutional Animal Care and Use Committee at the University of Florida. Mice were weaned at 3 weeks of age and given free access to water and standard diet containing 240 ppm iron (Teklad 7912, Harlan Laboratories). To induce iron deficiency, weanling mice were fed modified AIN-93G purified diet containing 2–6 ppm iron (Harlan Laboratories) for 3 weeks. Mice were genotyped by extracting genomic DNA from snipped tail samples (DNeasy Blood & Tissue Kit, Qiagen, Valencia, CA) and subjecting it to PCR analysis. To identify *Dmt1*$^{flox/flox}$ mice, we used primers F1: 5'-ATGGGCGAGTTAGAGGCTTT-3′ and R1: 5′-CCTGCATGTCAGAACCAATG-3′ (9). Cre-specific primers (forward: 5'-TTACCGGTCGATGCAACGAGT-3'; reverse: 5'-TTCCATGAGTGAACGAACCTGG-3') were used to detect the integration of the *Cre* gene into the mouse genome, and to identify *Dmt1*$^{liv/liv}$ mice. Primers F1 and R2: 5′-TTCTCTTGGGACAATCTGGG-3' (9) were used to confirm Cre-mediated excision in the liver. *Trf*$^{hpx/hpx}$ mice were identified at birth by their pallor and small size, and for survival, were injected intraperitoneally with human apo-transferrin (EMD Chemicals, Gibbstown, NJ), 0.1 mL of 6 mg/mL at 4 days of age, 0.2 mL in the second week, and 0.3 mL weekly until 14 weeks of age. *Dmt1*$^{flox/flox}$ and *Dmt1*$^{liv/liv}$ mice were crossed with *Hfe*$^{-/-}$ and *Trf*$^{hpx/hpx}$ mice to produce double-mutant strains along with single-mutant strains on the same genetic background.

RNA extraction and quantitative reverse transcriptase PCR

Total RNA was isolated from tissues by using RNAzol RT reagent (Molecular Research Center, Cincinnati, OH). Quantitative RT-PCR was used to measure mRNA levels as described previously (21). Mouse *Dmt1* mRNA levels were measured by using forward primer 5'- TCCTCATCACCATCGCA-GACACTT -3' and reverse primer 5'-TCCAAACGTGAGGGCCATGATAGT -3', which recognize all four known *Dmt1* transcript variants. *Dmt1* mRNA levels were normalized to ribosomal protein L13a (*Rpl13a*) mRNA levels, measured by using forward primer 5'- GCAAGTTCACAGAGGTCCTCAA -3' and reverse primer 5'- GGCATGAGGCAAACAGTCTTTA -3'.

Western blot analysis

Crude membrane fractions were isolated for the measurement of DMT1, TfR1, and TfR2 levels. Liver samples were homogenized by Dounce homogenization in ice-cold HEM buffer (20 mM HEPES, 1 mM EDTA, 200 mM mannitol, pH 7.4) containing 1× Complete, Mini Protease Inhibitor Cocktail (Roche, Indianapolis, IN). The homogenate was centrifuged at 10,000 x *g* for 10 minutes at 4 °C to remove insoluble cell debris. The supernatant was then centrifuged at 100,000 x *g* for 30 minutes at 4 °C to pellet the membranes, which were resuspended in HEM buffer. For measuring ZIP14 levels, tissue homogenates were used. Western analysis for DMT1, TfR1, and ZIP14 was performed as described previously (22). For TfR2, rabbit anti-TfR2 antibody (1:2500, Santa Cruz Biotechnology) was used.

Iron status parameters

Hemoglobin, plasma iron, transferrin saturation, and liver iron concentrations were determined as reported previously (21, 23). Formalin-fixed liver sections were deparaffinized and stained for ferric iron deposits by using Perls' Prussian blue stain.

Measurement of TBI and NTBI uptake

For TBI uptake, *Dmt1*$^{liv/liv}$ and *Dmt1*$^{flox/flox}$ mice were administered 150 μg of ^{59}Fe-transferrin (2 μCi) intravenously. After 2 hours, mice were sacrificed and whole-body counts per minute (cpm) were measured by using a Perkin Elmer Wizard^2 gamma counter. Immediately thereafter, individual tissues were harvested and cpm were determined. Tissue uptake of ^{59}Fe from transferrin was calculated as a percentage of whole-body cpm. NTBI uptake was determined by using the method of Craven et al. (24). Briefly, mice were administered 70 μg ferric citrate via tail vein injection to transiently saturate plasma transferrin. After 10 minutes, ^{59}Fe-labeled ferric citrate (2 μCi) was administered intravenously. Two hours later, animals were sacrificed and whole-body and tissue cpm were determined to calculate percentage NTBI uptake.

Statistical analysis

Data represent means ± standard error (SE). Means were compared by Student's unpaired *t* test or one-way ANOVA with Tukey's post-hoc test as appropriate (GraphPad Prism). A *P*-value < 0.05 was considered statistically significant.

RESULTS

Inactivation of Dmt1 specifically in the liver

Mice with *Dmt1* inactivated specifically in hepatocytes (*Dmt1*$^{liv/liv}$) were generated from an intercross of mice harboring a *loxP*-flanked (floxed) *Dmt1* allele (*Dmt1*$^{flox/flox}$) (9) and mice expressing an albumin-Cre transgene under control of the liver-specific albumin promoter (25). In the *Dmt1*$^{flox/flox}$ mice, the *loxP* recombination sites flanked exons 6–8 of the *Dmt1* gene (Fig. 1A) (9). Cre-mediated excision of the *loxP*-flanked region specifically in liver was confirmed by using PCR and primers F1, R1, and R2 (Fig. 1A, B). Quantitative RT-PCR analysis demonstrated that hepatic *Dmt1* mRNA levels at 8 weeks of age were > 90% lower in *Dmt1*$^{liv/liv}$ mice than in *Dmt1*$^{flox/flox}$ controls (Fig. 1C). By contrast, *Dmt1* mRNA levels were unaffected in heart or kidney of *Dmt1*$^{liv/liv}$ mice, indicating that *Dmt1* mRNA levels are not affected in extrahepatic tissues. Western blot analysis of crude liver membrane detected DMT1 in *Dmt1*$^{flox/flox}$ mice, but not in *Dmt1*$^{liv/liv}$ mice (Fig. 1D), thus confirming inactivation of hepatic *Dmt1*. Similar to previous reports (9), DMT1 in mouse liver was detected as a diffuse immunoreactive band at ~70 kDa. Transcript levels of hepatic DMT1 were measured at 3, 4, 8, 12, and 16 weeks of age and confirmed that liver *Dmt1* was inactivated throughout the duration of the studies (data not shown).

Liver-specific inactivation of Dmt1 has no effect on hepatic iron levels or body iron status

Compared with *Dmt1*$^{flox/flox}$ mice, *Dmt1*$^{liv/liv}$ mice appeared normal and displayed no abnormalities in iron status parameters at 8 weeks of age (Table 1). Hepatic total iron levels

as well as non-heme iron levels, an indicator of iron stores, were unaffected by liver-specific inactivation of *Dmt1*. Body weights, liver weights, and relative liver weights (% body weight) also did not differ between groups (data not shown).

Liver-specific inactivation of Dmt1 in $Hfe^{-/-}$ mice or $Trf^{hpx/hpx}$ mice does not affect hepatic iron loading or body iron status

To determine if DMT1 is required for hepatic iron accumulation, we crossed $Dmt1^{liv/liv}$ mice with $Hfe^{-/-}$ and $Trf^{hpx/hpx}$ mice to generate double-mutant $Hfe^{-/-};Dmt1^{liv/liv}$ and $Trf^{hpx/hpx};Dmt1^{liv/liv}$ mice, along with their respective controls ($Hfe^{-/-};Dmt1^{flox/flox}$ and $Trf^{hpx/hpx};Dmt1^{flox/flox}$ mice). Hepatic *Dmt1* mRNA levels in double-mutant $Dmt1^{liv/liv}$ mice were >90% lower than in the $Dmt1^{flox/flox}$ controls (data not shown). To allow for development of iron overload, double-mutant mice were examined at 16 weeks of age along with sets of single-mutant $Dmt1^{flox/flox}$ and $Dmt1^{liv/liv}$ mice generated on the same genetic background. We found that hepatic non-heme iron concentrations were ~3-fold higher in $Hfe^{-/-};Dmt1^{flox/flox}$ mice than $Dmt1^{flox/flox}$ mice (Fig. 2A). However, hepatic non-heme iron concentrations in $Hfe^{-/-};Dmt1^{liv/liv}$ mice did not differ from those in $Hfe^{-/-};Dmt1^{flox/flox}$ mice (Fig. 2A), indicating that DMT1 is dispensable for hepatic iron accumulation in $Hfe^{-/-}$ mice. Liver-specific inactivation of *Dmt1* also had no effect on the elevated plasma iron concentrations and transferrin saturations in $Hfe^{-/-}$ mice (Fig. 2B, C). Perls' Prussian blue staining of liver sections revealed prominent stainable iron in periportal hepatocytes in $Hfe^{-/-}$ mice but no differences between $Hfe^{-/-};Dmt1^{flox/flox}$ and $Hfe^{-/-};Dmt1^{liv/liv}$ mice (Fig. 2D). Notable iron staining was also sometimes observed in hepatocytes surrounding the central vein (data not shown), similar to a previous study of $Hfe^{-/-}$ mice (26). These observations indicate that DMT1 is dispensable for iron accumulation in hepatocytes in $Hfe^{-/-}$ mice.

Hypotransferrinemic mice ($Trf^{hpx/hpx}$) represent a more severe form of iron overload than $Hfe^{-/-}$ mice (19). At 16 weeks of age, hepatic non-heme iron concentrations in $Trf^{hpx/hpx};Dmt1^{flox/flox}$ mice were ~11-fold higher than those in control $Dmt1^{flox/flox}$ mice (Fig. 3A) and at least 2 times the level in $Hfe^{-/-}$ mice (Fig. 2A). Similar to $Hfe^{-/-};Dmt1^{liv/liv}$ mice, inactivation of *Dmt1* in $Trf^{hpx/hpx}$ mice had no effect on hepatic non-heme iron accumulation (Fig. 3A) or stainable iron in the liver (Fig. 3D). Hemoglobin and plasma iron levels also did not differ between $Trf^{hpx/hpx};Dmt1^{liv/liv}$ and $Trf^{hpx/hpx};Dmt1^{flox/flox}$ mice (Fig. 3B, C).

Effect of liver-specific inactivation of Dmt1 on NTBI and TBI uptake by the liver

To determine if hepatic DMT1 is required for the uptake of NTBI or TBI by the liver, we injected ^{59}Fe-labeled NTBI or ^{59}Fe-transferrin intravenously into $Dmt1^{liv/liv}$ and $Dmt1^{flox/flox}$ mice and measured ^{59}Fe uptake by the liver 2 hours later. As negative controls, we measured ^{59}Fe uptake by other organs that are known to take up NTBI. Similar to previous studies (27), NTBI was taken up most avidly by the liver, followed by the kidney, pancreas, and heart (Fig. 4A). However, NTBI uptake by the liver of $Dmt1^{liv/liv}$ mice did not differ from that of control $Dmt1^{flox/flox}$ mice, indicating that hepatocyte DMT1 is dispensable for NTBI clearance by the liver. By contrast, the uptake of TBI by the liver was 40% lower in $Dmt1^{liv/liv}$ mice compared with $Dmt1^{flox/flox}$ mice (Fig. 4B), revealing that

hepatocyte DMT1 is partially required for the hepatic uptake of iron from plasma transferrin. The effect was specific for liver because TBI uptake was unaffected in kidney, pancreas, or heart of *Dmt1*$^{liv/liv}$ mice. To determine if the lower hepatic TBI uptake by *Dmt1*$^{liv/liv}$ mice represents a delay in the clearance of plasma TBI, which may resolve at a later time, we measured the percentage of ^{59}Fe in the plasma 2 and 24 hours after injection. By 2 hours, the percentage of ^{59}Fe in the plasma did not differ between *Dmt1*$^{flox/flox}$ and *Dmt1*$^{liv/liv}$ mice (P=0.11) (Fig. 4C), and by 24 hours, very little ^{59}Fe was detectable in the plasma. These data indicate that the lower hepatic TBI uptake by *Dmt1*$^{liv/liv}$ mice does not represent a delay in the clearance of plasma TBI. The percentage of ^{59}Fe in the blood and spleen also did not differ at either time point, suggesting that iron uptake into developing erythroid cells was unaffected in *Dmt1*$^{liv/liv}$ mice.

Effect of liver-specific inactivation of Dmt1 on levels of hepatic TfR1, TfR2, and ZIP14

Although the lower hepatic TBI uptake in *Dmt1*$^{liv/liv}$ mice appears to be directly due to inactivation of *Dmt1*, it is possible that it results from a secondary effect on other proteins implicated in TBI uptake. It is equally possible that the lack of an effect of hepatic *Dmt1* inactivation on NTBI uptake is due to compensatory responses in other proteins involved in NTBI uptake. We therefore measured the levels of TfR1, TfR2, and ZIP14, which may also participate in TBI/NTBI uptake (28, 29). Western blot analysis revealed that the levels of these proteins did not differ between *Dmt1*$^{flox/flox}$ and *Dmt1*$^{liv/liv}$ mice (Fig. 5A–C).

Effect of liver-specific inactivation of Dmt1 on iron status and TBI uptake during iron deficiency

To determine if hepatocyte DMT1 is required to maintain iron status during iron deficiency, we compared iron status parameters of *Dmt1*$^{flox/flox}$ and *Dmt1*$^{liv/liv}$ mice that were fed iron-deficient diets. After 3 weeks, mice became iron deficient as compared with control (*Dmt1*$^{flox/flox}$) mice fed standard diet (Fig. 6A–D). However, no differences were observed between iron-deficient *Dmt1*$^{flox/flox}$ and *Dmt1*$^{liv/liv}$ mice. TBI uptake by the liver of *Dmt1*$^{flox/flox}$ mice was higher in iron-deficient animals compared with controls (36% vs. 30%, respectively, $P < 0.05$) (Fig. 6E). By contrast, TBI uptake by the liver of *Dmt1*$^{liv/liv}$ mice was not higher in iron-deficient animals compared to controls, suggesting that DMT1 is required for the enhanced TBI uptake into an iron-deficient liver.

Localization of DMT1 in liver

Confocal immunofluorescence microscopy was used to localize DMT1 in the liver. Human liver was used instead of mouse liver because immunofluorescence staining of mouse tissue was too weak to allow for reliable localization. DMT1 in hepatocytes displayed intracellular punctate staining with little, if any, staining plasma membrane (Supporting Fig. 1).

DISCUSSION

The finding that liver iron levels were unaffected in *Dmt1*$^{liv/liv}$ mice indicates that hepatocyte DMT1 is dispensable for the overall iron economy of the liver. In addition, the observation that hepatic iron accumulation and deposition of iron in hepatocytes were unaffected in double-mutant *Hfe*$^{-/-}$;*Dmt1*$^{liv/liv}$ and *Trf*$^{hpx/hpx}$;*Dmt1*$^{liv/liv}$ mice demonstrates

that hepatocyte DMT1 is not required for the development of hepatic iron overload characteristic of hemochromatosis or hypotransferrinemia. Furthermore, no alterations were found in the levels of plasma iron, total iron-binding capacity, transferrin saturation, or hemoglobin in single- or double-mutant *Dmt1*$^{liv/liv}$ mice, suggesting that inactivation of hepatocyte DMT1 does not affect systemic iron metabolism.

The first clue that DMT1 was dispensable for hepatic iron accumulation was provided by studies of the *Dmt1*$^{-/-}$ mouse, which found that *Dmt1*$^{-/-}$ neonates had 3 times normal liver iron levels (9). This observation, however, was confounded by the fact that the *Dmt1*$^{-/-}$ mice had severe anemia and prominent extramedullary erythropoiesis in the liver. Hepatic iron accumulation in *Dmt1*$^{-/-}$ mice was directly investigated by administering a single intraperitoneal dose of 5 mg of iron dextran (9). The iron dextran injection resulted in a large increase in the levels of liver iron, in hepatocytes as well as macrophages. Although these observations indicated that an intraperitoneal injection of a pharmacologic dose of iron (in a non-physiological form) could load iron into the liver in the absence of DMT1, it is unclear how relevant these data are to usual pathways of hepatic iron uptake and accumulation. Therefore, in the present study we assessed the role of DMT1 in hepatic iron uptake by intravenously administering physiologic forms of iron—transferrin or ferric citrate as NTBI (18)—and by using animal models of human disorders of iron overload.

Similar to *HFE*-related hemochromatosis patients, *Hfe*$^{-/-}$ mice hyperabsorb dietary iron and deposit the excess in hepatocytes, starting with periportal hepatocytes (3). Here we observed a similar pattern of iron deposition in the liver of *Hfe*$^{-/-}$ mice lacking hepatocyte DMT1 (*Hfe*$^{-/-}$;*Dmt1*$^{liv/liv}$), indicating that DMT1 is dispensable for hepatocyte iron accumulation in this animal model. Also similar to hemochromatosis patients, *Hfe*$^{-/-}$ mice have elevated levels of plasma NTBI, even when transferrin is not fully saturated (12). Most plasma NTBI is rapidly cleared by hepatocytes and is therefore believed to be a significant contributor to hepatic iron deposition (11, 12). If so, our studies suggest that hepatocyte DMT1 is not required for NTBI uptake because hepatic iron levels were similar in *Hfe*$^{-/-}$ mice with or without hepatocyte DMT1. The likelihood that hepatocyte DMT1 is dispensable for the hepatic uptake of NTBI is strongly supported by our observation that hepatic iron accumulation and iron deposition in hepatocytes were unaffected in *Trf*$^{hpx/hpx}$ mice lacking hepatocyte DMT1 (*Trf*$^{hpx/hpx}$;*Dmt1*$^{liv/liv}$ mice). Due to a mutation in the *Trf* locus, *Trf*$^{hpx/hpx}$ mice do not express normal transferrin mRNA and therefore have effectively no plasma transferrin (19). As a consequence, most iron in the plasma of *Trf*$^{hpx/hpx}$ mice is NTBI.

NTBI has been recognized as a contributor to hepatic iron overload for more than 25 years (24), but the molecular mechanisms involved have proved elusive (11). A possible role for DMT1 in hepatic NTBI uptake was first proposed in 2000 by Trinder et al. (17), who found by using immunohistochemistry that DMT1 was present on rat hepatocyte plasma membranes and that DMT1 levels were elevated in iron overload. DMT1 levels were also reported to be upregulated in isolated hepatocytes from *Hfe*$^{-/-}$ mice, which had elevated levels of plasma NTBI (12). Support for DMT1 in NTBI uptake has been additionally provided by cell culture studies showing that transfection of hepatoma cells with DMT1 cDNA increased DMT1 levels at the plasma membrane and enhanced the uptake of NTBI

(15). Since these initial reports, numerous studies (14, 30, 31) and recent reviews (5, 11, 13) cite DMT1 as the major mediator of hepatic NTBI uptake.

In the present study, we formally tested the hypothesis that hepatocyte DMT1 plays a role in NTBI uptake by measuring the hepatic uptake of radiolabeled NTBI injected into *Dmt1*$^{liv/liv}$ mice. Our finding that NTBI uptake into the liver was unaffected in *Dmt1*$^{liv/liv}$ mice provides clear evidence that hepatocyte DMT1 is dispensable for hepatic NTBI uptake; it also demonstrates that at least one alternative hepatic NTBI uptake pathway must exist. Other proteins that have been implicated in NTBI uptake include ZIP14 (28, 32), ZIP8 (33), TfR2 (34), L-type voltage-gated calcium channels (35), and lipocalin 2 (36). The observation that hepatic levels of ZIP14 and TfR2 were unaffected in *Dmt1*$^{liv/liv}$ mice suggests that NTBI uptake in the absence of hepatocyte DMT1 does not result from a compensatory upregulation of either of these proteins.

Although hepatocyte DMT1 is not required for hepatic uptake of NTBI, we found that it is partially required for the uptake of TBI, as revealed by the 40% lower TBI uptake by the liver in *Dmt1*$^{liv/liv}$ mice. The diminished TBI uptake likely reflects impaired uptake into hepatocytes, since transferrin iron is taken up nearly exclusively by hepatocytes rather than other cell types of the liver (37). Yet despite the lower TBI uptake, liver iron concentrations in *Dmt1*$^{liv/liv}$ mice were not lower than those in control animals. This observation suggests that DMT1-mediated iron uptake from plasma transferrin is not a major contributor to the normal pool of hepatic iron. Ferrokinetic studies of internal iron exchange in the rat have found that approximately 20% of the iron from intravenously injected ^{59}Fe-transferrin was taken up into the liver by 5 hours (4). Our studies in mice found a similar percentage of iron uptake from transferrin (i.e., about 25% by 2 hours post injection). The apparently minor contribution of DMT1-mediated transferrin-iron uptake to total hepatic iron levels is consistent with the low overall expression level of DMT1 in the liver compared to other tissues (6). The expression of TfR1 is also much lower in liver than in other tissues (38). Indeed, TfR1 is likely to be a minor contributor as well to hepatic iron levels because TfR1 binding sites on hepatocytes are saturated under normal physiologic concentrations of transferrin (39) and because transferrin iron is well known to be readily taken up by hepatocytes using a TfR1-independent pathway (40). On the other hand, hepatic DMT1 (and TfR1) would seem to become more important during iron deficiency, when their expression is up-regulated (22, 41). Consistent with this possibility, hepatic TBI uptake was higher in iron-deficient *Dmt1*$^{flox/flox}$ mice compared with controls. A role for DMT1 in this enhanced TBI uptake during iron deficiency is supported by the observation that no such increase in hepatic TBI uptake was observed in iron-deficient *Dmt1*$^{liv/liv}$ mice. However, the increase in hepatic uptake of TBI during iron deficiency was small (~6%) in *Dmt1*$^{flox/flox}$ mice and hepatic non-heme iron concentrations did not differ between iron-deficient *Dmt1*$^{flox/flox}$ and *Dmt1*$^{liv/liv}$ mice. It therefore appears that DMT1 is not required for the overall economy of the liver, even during iron deficiency.

Studies of DMT1 in iron-deficient liver are inconsistent. Trinder et al. (17) reported that DMT1 became undetectable in iron-deficient rat liver, whereas we found that DMT1 is markedly up-regulated in iron deficiency (22). The opposite results may reflect quantitation differences between immunohistochemistry (17) and Western blotting (22), but this seems

unlikely. Trinder et al. (17) also concluded that hepatocyte DMT1 localizes to the plasma membrane, whereas others report a predominantly cytosolic localization (15, 31). Our immunohistochemistry results indicate that DMT1 in human liver sections is intracellular and vesicular, and not readily detectable at the plasma membrane. The intracellular distribution of hepatocyte DMT1 suggests that the defect in TBI uptake by *Dmt1*$^{liv/liv}$ mouse liver is due to the lack of endosomal DMT1.

In conclusion, these studies reveal that hepatocyte DMT1 is not required for the overall iron economy of the liver, hepatic iron accumulation in genetic iron overload, or NTBI uptake by the liver. However, hepatocyte DMT1 does appear to be partially required for the liver to take up TBI. Further research will be needed to identify the molecular mechanisms of hepatic NTBI uptake and how they contribute to hepatic iron accumulation in iron overload disorders.

Supplementary Material

Refer to Web version on PubMed Central for supplementary material.

ACKNOWLEDGMENTS

We graciously thank the late Dr. Hiromi Gunshin and Dr. Nancy Andrews (Duke University School of Medicine, Durham, NC) for providing the mutant mice used in these studies. We are also grateful to Dr. Roniel Cabrera (University of Florida School of Medicine) for help with identifying liver structures.

Financial Support

This work was supported by National Institutes of Health Grant R01 DK080706 (to M.D.K.) and the ILSI North America Future Leader Award (to M.D.K.).

List of Abbreviations

DMT1	divalent metal-ion transporter-1
NTBI	non-transferrin-bound iron
TBI	transferrin-bound iron
TfR1	transferrin receptor 1
TfR2	transferrin receptor 2
SR-B1	scavenger receptor class B type I
ZIP14	ZRT/IRT-like protein 14

REFERENCES

1. Bothwell, TH.; Charlton, RW.; Cook, JD.; Finch, CA. Iron Metabolism in Man. Oxford: Blackwell Scientific Publications; 1979. p. 576
2. Pietrangelo A. Hereditary hemochromatosis: pathogenesis, diagnosis, and treatment. Gastroenterology. 2010; 139:393–408. [PubMed: 20542038]
3. Zhou XY, Tomatsu S, Fleming RE, Parkkila S, Waheed A, Jiang J, Fei Y, et al. HFE gene knockout produces mouse model of hereditary hemochromatosis. Proc Natl Acad Sci U S A. 1998; 95:2492–2497. [PubMed: 9482913]

4. Cheney BA, Lothe K, Morgan EH, Sood SK, Finch CA. Internal iron exchange in the rat. Am J Physiol. 1967; 212:376–380. [PubMed: 6018021]
5. Graham RM, Chua AC, Herbison CE, Olynyk JK, Trinder D. Liver iron transport. World J Gastroenterol. 2007; 13:4725–4736. [PubMed: 17729394]
6. Gunshin H, Mackenzie B, Berger UV, Gunshin Y, Romero MF, Boron WF, Nussberger S, et al. Cloning and characterization of a mammalian proton-coupled metal-ion transporter. Nature. 1997; 388:482–488. [PubMed: 9242408]
7. Fleming MD, Romano MA, Su MA, Garrick LM, Garrick MD, Andrews NC. Nramp2 is mutated in the anemic Belgrade (b) rat: evidence of a role for Nramp2 in endosomal iron transport. Proc Natl Acad Sci U S A. 1998; 95:1148–1153. [PubMed: 9448300]
8. Jandl JH, Inman JK, Simmons RL, Allen DW. Transfer of iron from serum iron-binding protein to human reticulocytes. J Clin Invest. 1959; 38:161–185. [PubMed: 13620780]
9. Gunshin H, Fujiwara Y, Custodio AO, Direnzo C, Robine S, Andrews NC. Slc11a2 is required for intestinal iron absorption and erythropoiesis but dispensable in placenta and liver. J Clin Invest. 2005; 115:1258–1266. [PubMed: 15849611]
10. Anderson GJ, Vulpe CD. Mammalian iron transport. Cell Mol Life Sci. 2009; 66:3241–3261. [PubMed: 19484405]
11. Brissot P, Ropert M, Le Lan C, Loreal O. Non-transferrin bound iron: A key role in iron overload and iron toxicity. Biochim Biophys Acta. 2012; 1820:403–410. [PubMed: 21855608]
12. Chua AC, Olynyk JK, Leedman PJ, Trinder D. Nontransferrin-bound iron uptake by hepatocytes is increased in the Hfe knockout mouse model of hereditary hemochromatosis. Blood. 2004; 104:1519–1525. [PubMed: 15155457]
13. Garrick MD, Garrick LM. Cellular iron transport. Biochim Biophys Acta. 2009; 1790:309–325. [PubMed: 19344751]
14. Mackenzie B, Ujwal ML, Chang MH, Romero MF, Hediger MA. Divalent metal-ion transporter DMT1 mediates both H+ -coupled Fe2+ transport and uncoupled fluxes. Pflugers Arch. 2006; 451:544–558. [PubMed: 16091957]
15. Shindo M, Torimoto Y, Saito H, Motomura W, Ikuta K, Sato K, Fujimoto Y, et al. Functional role of DMT1 in transferrin-independent iron uptake by human hepatocyte and hepatocellular carcinoma cell, HLF. Hepatol Res. 2006; 35:152–162. [PubMed: 16707273]
16. Sohn YS, Ghoti H, Breuer W, Rachmilewitz E, Attar S, Weiss G, Cabantchik ZI. The role of endocytic pathways in cellular uptake of plasma non-transferrin iron. Haematologica. 2012; 97:670–678. [PubMed: 22180428]
17. Trinder D, Oates PS, Thomas C, Sadleir J, Morgan EH. Localisation of divalent metal transporter 1 (DMT1) to the microvillus membrane of rat duodenal enterocytes in iron deficiency, but to hepatocytes in iron overload. Gut. 2000; 46:270–276. [PubMed: 10644324]
18. Grootveld M, Bell JD, Halliwell B, Aruoma OI, Bomford A, Sadler PJ. Non-transferrin-bound iron in plasma or serum from patients with idiopathic hemochromatosis Characterization by high performance liquid chromatography and nuclear magnetic resonance spectroscopy. J Biol Chem. 1989; 264:4417–4422. [PubMed: 2466835]
19. Trenor CC 3rd, Campagna DR, Sellers VM, Andrews NC, Fleming MD. The molecular defect in hypotransferrinemic mice. Blood. 2000; 96:1113–1118. [PubMed: 10910930]
20. Levy JE, Montross LK, Cohen DE, Fleming MD, Andrews NC. The C282Y mutation causing hereditary hemochromatosis does not produce a null allele. Blood. 1999; 94:9–11. [PubMed: 10381492]
21. Nam H, Knutson MD. Effect of dietary iron deficiency and overload on the expression of ZIP metal-ion transporters in rat liver. Biometals. 2012; 25:115–124. [PubMed: 21826460]
22. Nam H, Wang CY, Zhang L, Zhang W, Hojyo S, Fukada T, Knutson MD. ZIP14 and DMT1 in the liver, pancreas, and heart are differentially regulated by iron deficiency and overload: implications for tissue iron uptake in iron-related disorders. Haematologica. 2013 In Press.
23. Knutson MD, Walter PB, Ames BN, Viteri FE. Both iron deficiency and daily iron supplements increase lipid peroxidation in rats. J Nutr. 2000; 130:621–628. [PubMed: 10702595]

24. Craven CM, Alexander J, Eldridge M, Kushner JP, Bernstein S, Kaplan J. Tissue distribution and clearance kinetics of non-transferrin-bound iron in the hypotransferrinemic mouse: a rodent model for hemochromatosis. Proc Natl Acad Sci U S A. 1987; 84:3457–3461. [PubMed: 3472216]
25. Postic C, Shiota M, Niswender KD, Jetton TL, Chen Y, Moates JM, Shelton KD, et al. Dual roles for glucokinase in glucose homeostasis as determined by liver and pancreatic beta cell-specific gene knock-outs using Cre recombinase. J Biol Chem. 1999; 274:305–315. [PubMed: 9867845]
26. Fleming RE, Holden CC, Tomatsu S, Waheed A, Brunt EM, Britton RS, Bacon BR, et al. Mouse strain differences determine severity of iron accumulation in Hfe knockout model of hereditary hemochromatosis. Proc Natl Acad Sci U S A. 2001; 98:2707–2711. [PubMed: 11226304]
27. Bradbury MW, Raja K, Ueda F. Contrasting uptakes of 59Fe into spleen, liver, kidney and some other soft tissues in normal and hypotransferrinaemic mice. Influence of an antibody against the transferrin receptor. Biochem Pharmacol. 1994; 47:969–974. [PubMed: 8147916]
28. Liuzzi JP, Aydemir F, Nam H, Knutson MD, Cousins RJ. Zip14 (Slc39a14) mediates non-transferrin-bound iron uptake into cells. Proc Natl Acad Sci U S A. 2006; 103:13612–13617. [PubMed: 16950869]
29. Zhao N, Gao J, Enns CA, Knutson MD. ZRT/IRT-like protein 14 (ZIP14) promotes the cellular assimilation of iron from transferrin. J Biol Chem. 2010; 285:32141–32150. [PubMed: 20682781]
30. Bergmann OM, Mathahs MM, Broadhurst KA, Weydert JA, Wilkinson N, Howe JR, Han O, et al. Altered expression of iron regulatory genes in cirrhotic human livers: clues to the cause of hemosiderosis? Lab Invest. 2008; 88:1349–1357. [PubMed: 18838961]
31. Bardou-Jacquet E, Island ML, Jouanolle AM, Detivaud L, Fatih N, Ropert M, Brissot E, et al. A novel N491S mutation in the human SLC11A2 gene impairs protein trafficking and in association with the G212V mutation leads to microcytic anemia and liver iron overload. Blood Cells Mol Dis. 2011; 47:243–248. [PubMed: 21871825]
32. Pinilla-Tenas JJ, Sparkman BK, Shawki A, Illing AC, Mitchell CJ, Zhao N, Liuzzi JP, et al. Zip14 is a complex broad-scope metal-ion transporter whose functional properties support roles in the cellular uptake of zinc and nontransferrin-bound iron. Am J Physiol Cell Physiol. 2011; 301:C862–C871. [PubMed: 21653899]
33. Wang CY, Jenkitkasemwong S, Duarte S, Sparkman BK, Shawki A, Mackenzie B, Knutson MD. ZIP8 Is an Iron and Zinc Transporter Whose Cell-surface Expression Is Up-regulated by Cellular Iron Loading. J Biol Chem. 2012; 287:34032–34043. [PubMed: 22898811]
34. Graham RM, Reutens GM, Herbison CE, Delima RD, Chua AC, Olynyk JK, Trinder D. Transferrin receptor 2 mediates uptake of transferrin-bound and non-transferrin-bound iron. J Hepatol. 2008; 48:327–334. [PubMed: 18083267]
35. Otto-Duessel M, Brewer C, Wood JC. Interdependence of cardiac iron and calcium in a murine model of iron overload. Transl Res. 2011; 157:92–99. [PubMed: 21256461]
36. Huang H, Akira S, Santos MM. Is the iron donor lipocalin 2 implicated in the pathophysiology of hereditary hemochromatosis? Hepatology. 2009; 49:1012–1016. [PubMed: 19152427]
37. Morgan EH, Smith GD, Peters TJ. Uptake and subcellular processing of 59Fe-125I–labelled transferrin by rat liver. Biochem J. 1986; 237:163–173. [PubMed: 3800875]
38. Fleming RE, Migas MC, Holden CC, Waheed A, Britton RS, Tomatsu S, Bacon BR, et al. Transferrin receptor 2: continued expression in mouse liver in the face of iron overload and in hereditary hemochromatosis. Proc Natl Acad Sci U S A. 2000; 97:2214–2219. [PubMed: 10681454]
39. Trinder D, Morgan E, Baker E. The mechanisms of iron uptake by fetal rat hepatocytes in culture. Hepatology. 1986; 6:852–858. [PubMed: 3758939]
40. Trinder D, Zak O, Aisen P. Transferrin receptor-independent uptake of differic transferrin by human hepatoma cells with antisense inhibition of receptor expression. Hepatology. 1996; 23:1512–1520. [PubMed: 8675172]
41. Masaratana P, Patel N, Latunde-Dada GO, Vaulont S, Simpson RJ, McKie AT. Regulation of iron metabolism in Hamp (−/−) mice in response to iron-deficient diet. Eur J Nutr. 2012

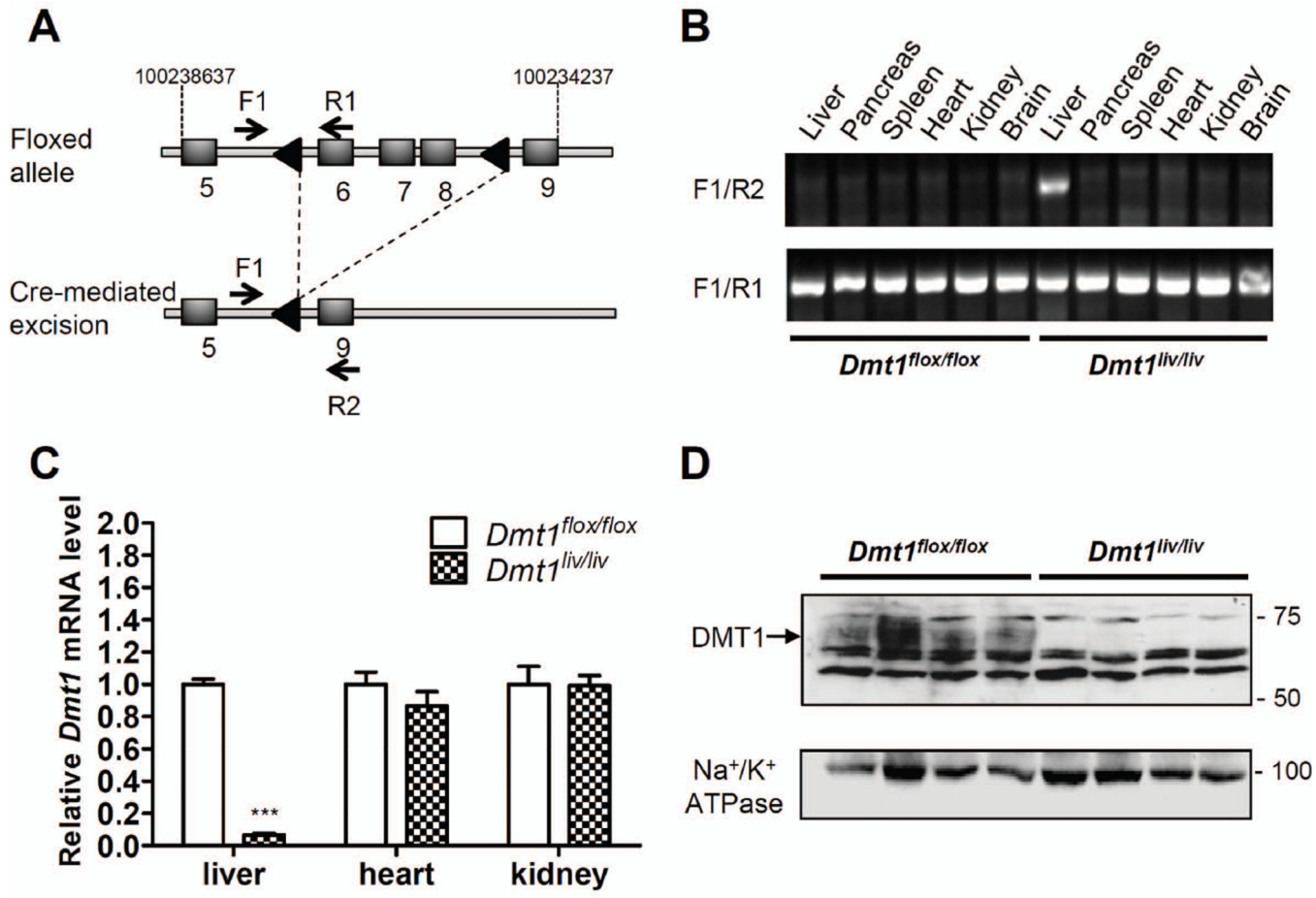

Fig. 1.

Disruption of *Dmt1* in mouse liver. (A) Schematic depictions of the *loxP*-flanked (floxed) *Dmt1* allele and the allele after Cre recombinase-mediated excision. F1, R1, and R2 indicate forward (F) and reverse (R) primers used for PCR genotyping. Arrowheads denote *loxP* sites and shaded boxes indicate exons located between positions 10023867 and 10023437 on chromosome 15. (B) PCR analysis of genomic DNA extracted from tissues of mice at 8 weeks of age. (C) Relative *Dmt1* mRNA levels in liver, heart, and kidney as determined by using quantitative RT-PCR with *Rpl13a* as an internal control gene. Values represent mean ± SE, n=3–4, ***$P < 0.001$. (D) Western blot analysis of DMT1 in crude membrane fractions isolated from livers of $Dmt1^{flox/flox}$ and $Dmt1^{liv/liv}$ mice. All analyses were performed on samples from 8-week-old mice.

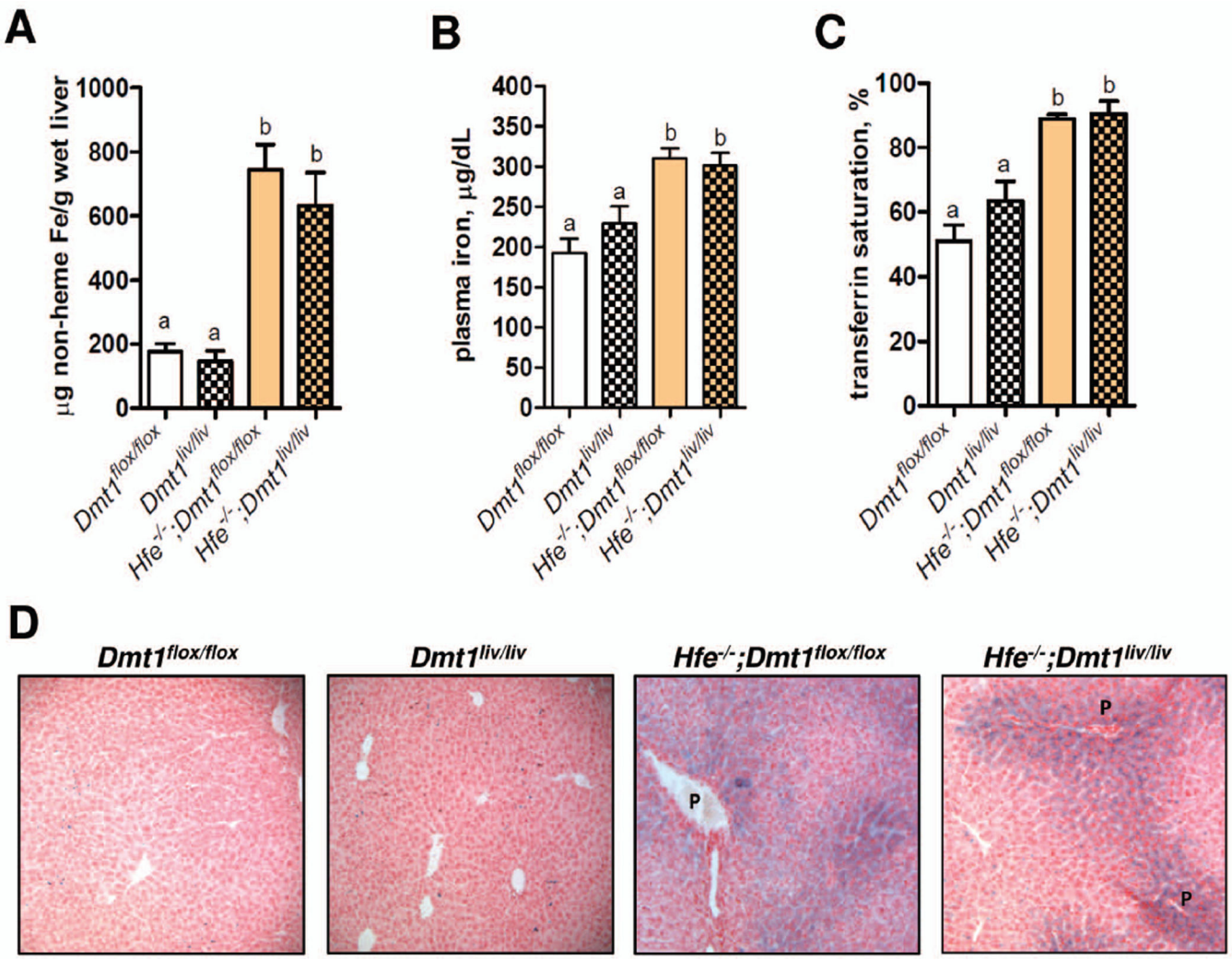

Fig. 2.

Hepatic iron accumulation, plasma iron levels, and transferrin saturation are not affected by liver-specific inactivation of *Dmt1* in *Hfe* knockout ($Hfe^{-/-}$) mice. (A) Hepatic non-heme iron concentrations were determined colorimetrically after acid digestion of tissues. (B) Plasma iron and (C) transferrin saturation were determined by using standard methods. Values represent mean ± SE, n=6. Means without a common superscript differ significantly ($P < 0.05$). (D) Histological examination of iron loading in the liver by using Perls' Prussian blue to stain for iron. Branches of the portal vein (P) are indicated. All analyses were performed on samples from 16-week-old mice.

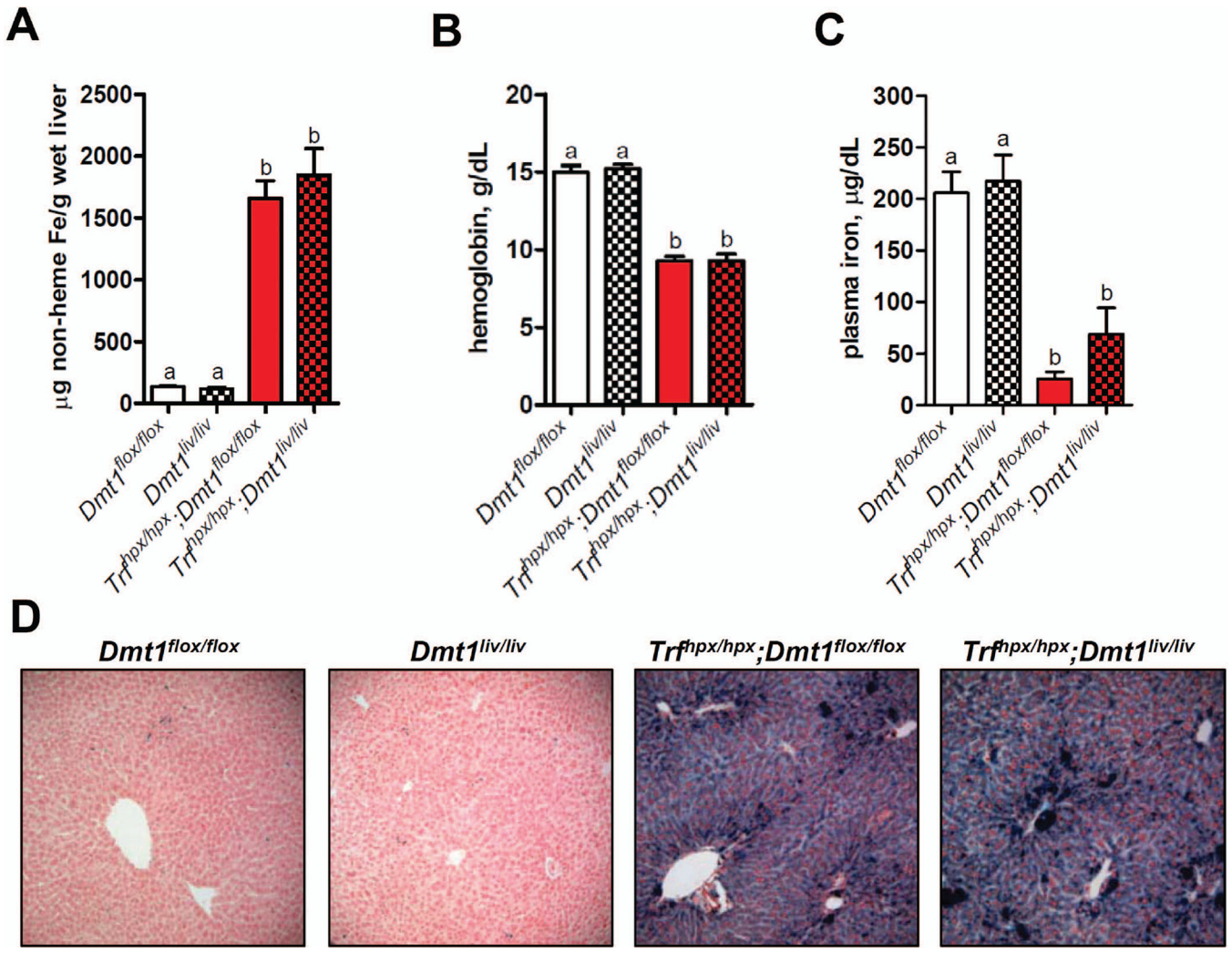

Fig. 3.

Hepatic iron accumulation, hemoglobin levels, and plasma iron levels are not affected by liver-specific inactivation of *Dmt1* in hypotransferrinemic (*Trf* $^{hpx/hpx}$) mice. (A) Hepatic non-heme iron concentrations were determined colorimetrically after acid digestion of tissues. (B) Hemoglobin and (C) plasma iron levels were determined by using standard methods. Values represent mean ± SE, n=6, except for hemoglobin levels in (*Trf* $^{hpx/hpx}$) mice (n=3–4). Means without a common superscript differ significantly ($P < 0.05$). (D) Histological examination of iron loading in the liver by using Perls' Prussian blue to stain for iron. All analyses were performed on samples from 16-week-old mice.

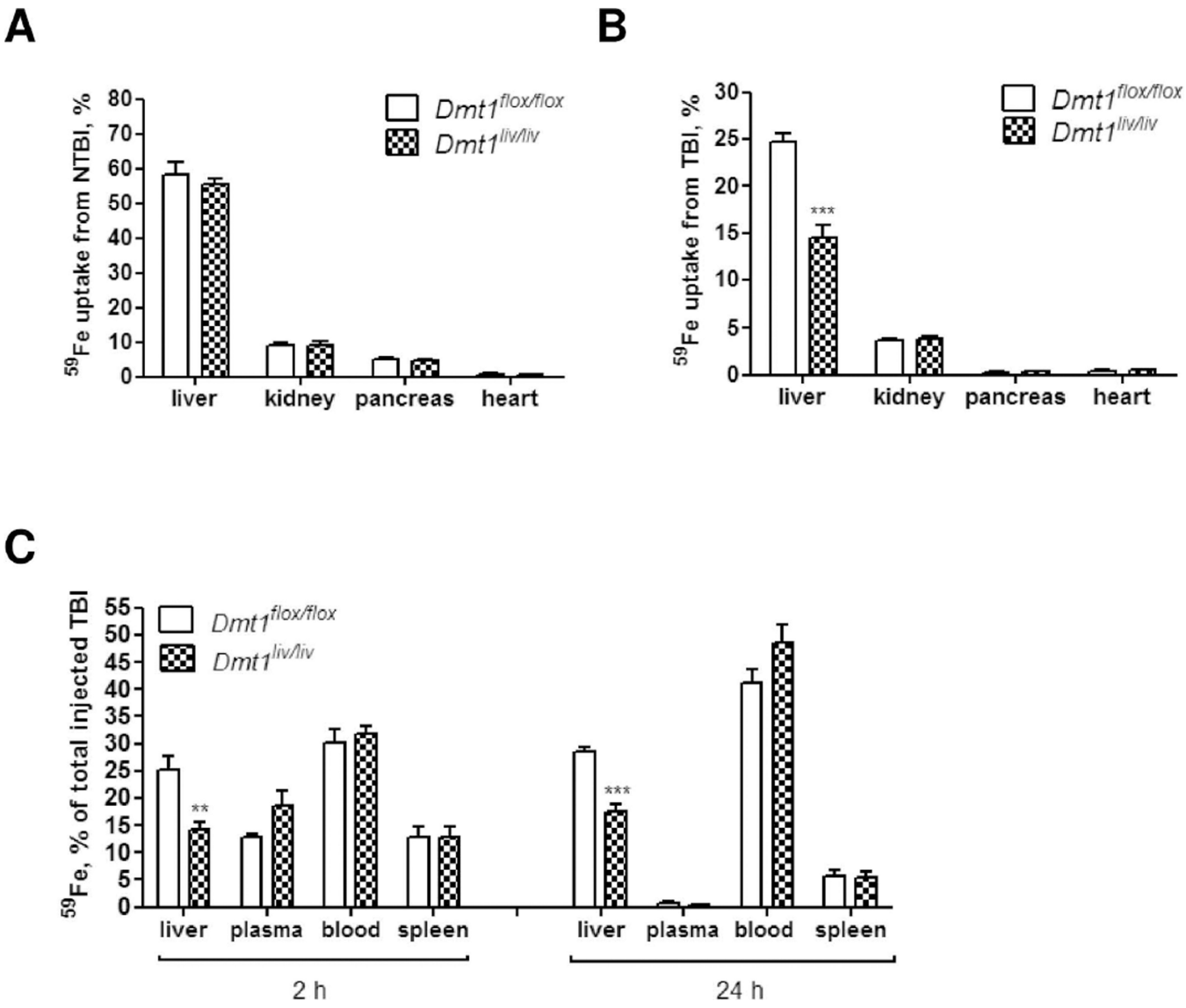

Fig. 4.

Tissue uptake of ^{59}Fe from NTBI or TBI injected into the plasma of *Dmt1*$^{flox/flox}$ and *Dmt1*$^{liv/liv}$ mice. (A) NTBI uptake by the liver (n=10), kidney (n=5), pancreas (n=5), and heart (n=5). Mice were injected with ferric citrate to transiently saturate plasma transferrin and then ^{59}Fe-labeled ferric citrate was injected 10 minutes later. After 2 hours, mice were sacrificed and whole-body and tissue ^{59}Fe cpm were measured by gamma counting. Tissue uptake of ^{59}Fe from NTBI was calculated as a percentage of whole-body cpm. (B) TBI uptake by the liver (n=14), kidney (n=6), pancreas (n=6), and heart (n=6). Mice were injected with ^{59}Fe-transferrin and sacrificed after 2 hours. Whole-body and tissue ^{59}Fe cpm were determined by gamma counting. Tissue uptake of ^{59}Fe from TBI was calculated as a percentage of whole-body cpm. (C) Distribution of ^{59}Fe among liver, plasma, blood, and spleen 2 and 24 hours after injecting mice with ^{59}Fe-transferrin (n=5–6 at each time point). Results are expressed as mean ± SE. All measurements were performed on mice at 7–8 weeks of age.

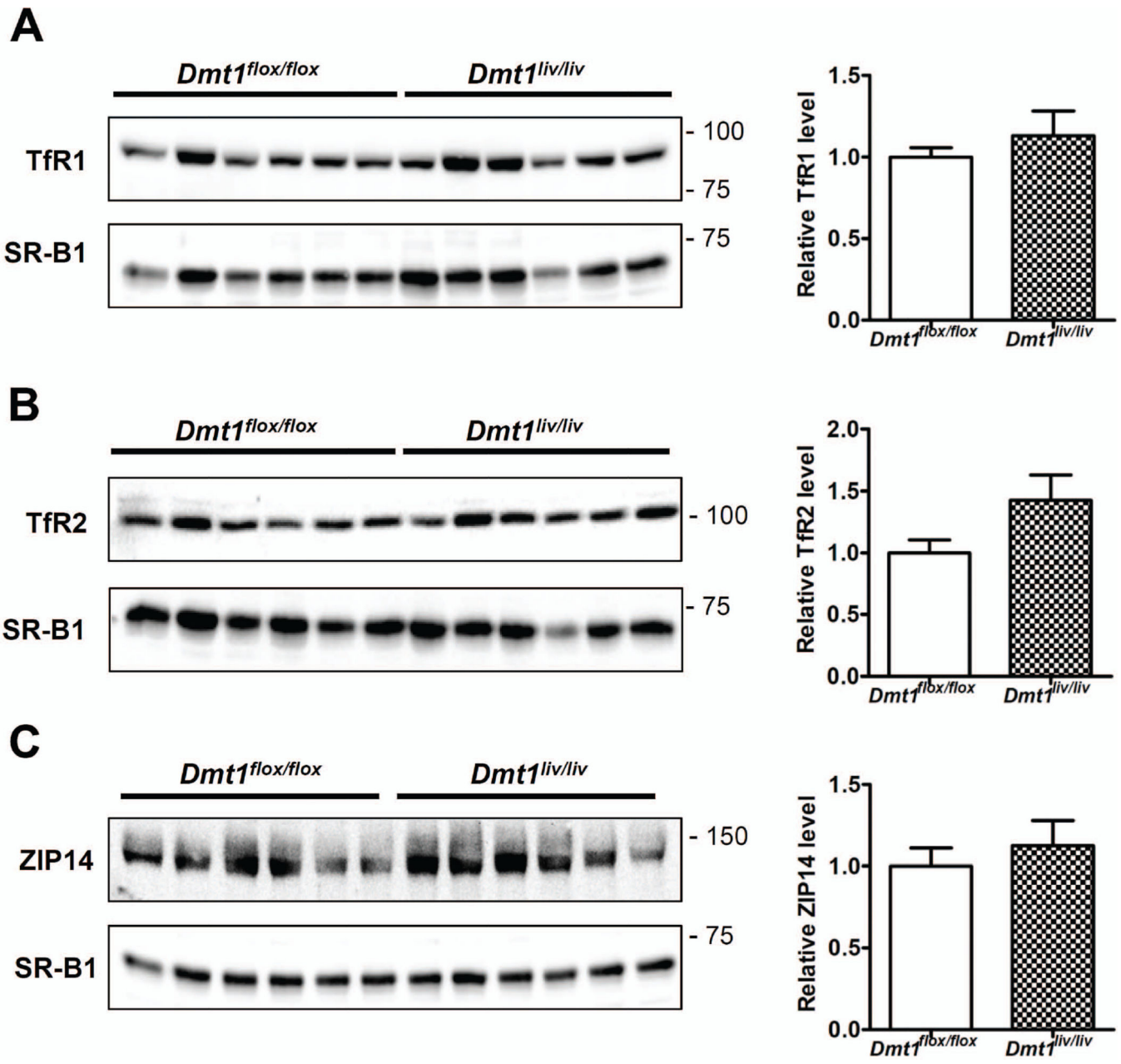

Fig. 5.

Effect of liver-specific inactivation of *Dmt1* on hepatic levels of TfR1, TfR2, and ZIP14 (A–C) Western blot analyses of TfR1, TfR2, and ZIP14 in $Dmt1^{liv/liv}$ mice and controls ($Dmt1^{flox/flox}$). Blots were stripped and reprobed for SR-B1 as a lane loading control. Relative band intensities determined by densitometry and normalized to SR-B1. Values represent mean ± SE, n=6. All analyses were performed on samples from 8-week-old mice.

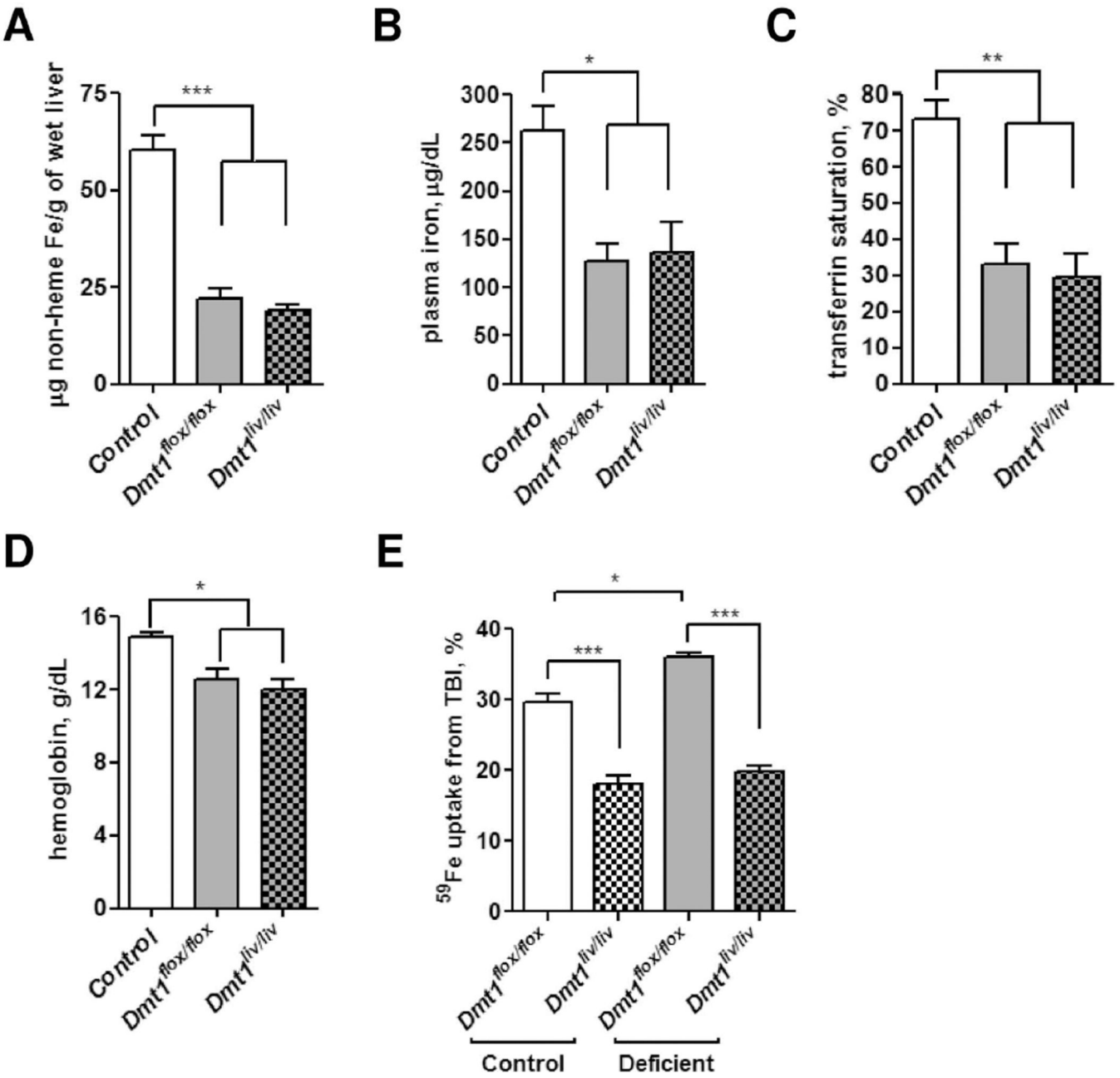

Fig. 6.

Effect of liver-specific inactivation of *Dmt1* on iron status and TBI uptake during iron deficiency. *Dmt1*$^{flox/flox}$ and *Dmt1*$^{liv/liv}$ mice were fed iron-deficient diet for 3 weeks to induce iron deficiency. Control values were obtained from age-matched *Dmt1*$^{flox/flox}$ mice fed with standard rodent diet for 3 weeks. Iron status was assessed by measuring (A) hepatic non-heme iron concentrations (B) plasma iron concentrations (C) transferrin saturation, and (D) hemoglobin. (E) TBI uptake by the liver in normal and iron-deficient conditions. Mice were injected with ^{59}Fe-transferrin and sacrificed after 2 hours. Whole-body and tissue ^{59}Fe cpm were determined by gamma counting. Tissue uptake of ^{59}Fe from TBI was calculated

as a percentage of whole-body cpm. Values represent mean ± SE, n=3. All analyses were performed on mice at 6 weeks of age.

Table 1

Iron status parameters of *Dmt1*$^{flox/flox}$ and *Dmt1*$^{liv/liv}$ mice

Parameter	Unit	*Dmt1*$^{flox/flox}$	*Dmt1*$^{liv/liv}$	*n*	*P*
Hemoglobin	g/dL	15.30 ± 0.33	15.18 ± 0.47	6	0.843
Plasma iron	μg/dL	270.3 ± 17.72	283.5 ± 14.44	6	0.575
TIBC	μg/dL	372.6 ± 15.01	375.0 ± 27.72	4–5	0.938
Transferrin saturation	%	72.36 ± 4.25	73.88 ± 3.69	4–5	0.802
Hepatic iron	μg Fe/g	796.7 ± 65.08	885.0 ± 12.66	3	0.254
Hepatic non-heme iron	μg Fe/g	132.1 ± 22.24	125.9 ± 26.24	6	0.861

TIBC, total iron-binding capacity. Hepatic iron (heme and non-heme) levels were determined by ICP-MS, and are reported as μg Fe/g of tissue dry weight. Hepatic non-heme iron levels were measured colorimetrically and are reported as μg Fe/g of tissue wet weight. Values are means ± SE. Measurements were at 8 weeks of age. *P* values were obtained by using Student's *t* test.